Flow Measurement and Instrumentation 73 (2020) 101739

Contents lists available at ScienceDirect

Flow Measurement and Instrumentation

journal homepage: http://www.elsevier.com/locate/flowmeasinst

A novel approach based on artificial neural network for calibration of multi-hole pressure probes

Homam Nikpey Somehsaraei [a,**], Magnus Hölle [b], Herwart Hönen [b], Mohsen Assadi [a]

[a] Department of Energy and Petroleum Engineering, University of Stavanger, 4036, Stavanger, Norway
[b] Institute of Jet Propulsion and Turbomachinery, RWTH Aachen University, Templergraben 55, Aachen, 52062, Germany

ARTICLE INFO

Keywords:
Pressure probe
Polynomial approach
ANN
Calibration

ABSTRACT

Imperfections in the manufacturing process of flow measuring probes affect their measuring behavior. Nevertheless, in order to provide the highest possible accuracy, each individual multi-hole pressure probe has to be calibrated before using them in turbomachinery. This paper presents a novel method based on artificial neural networks (ANN) to predict the flow parameters of multi-hole pressure probes. A two-stage ANN approach using multilayer perceptron (MLP) is proposed in this study. The two-stage prediction approach involves two MLP networks, which represent the calibration data and the prediction error. For a given set of inputs, outputs from both networks are combined to estimate the measured value. The calibration data of a 5-hole probe at RWTH Aachen was used to develop and validate the proposed ANN models and two-stage prediction approach. The results showed that the ANN can predict the flow parameters with high accuracy. Using the two-stage approach, the prediction accuracy was further improved compared to polynomial functions, i.e. a commonly used method in probe calibration. Furthermore, the proposed approach offers high interpolation capabilities while preventing overfitting (i.e. failure to fit new data). Unlike polynomials, it is shown that the ANN based method can provide accurate predictions at intermediate points without large oscillations.

1. Introduction

The determination of the three-dimensional steady flow properties in a turbomachine requires information about Mach number, total pressure and the flow angles in yaw and pitch direction. Pneumatic multi-hole probes (e.g. 4-hole or 5-hole probes) are commonly applied instruments for the measurement of the 3D flow vectors. The crucial design criteria for these probe types are the measuring characteristics, which have to provide an unambiguous assignment of the pressure readings to the spatial flow properties.

The example of a 5-hole probe with spherical head as shown in Fig. 1 demonstrates that the pressure readings of bores 1 and 3 are sensitive for angle variations in horizontal direction (yaw) and those of bores 2 and 4 indicate angle variations in vertical direction (pitch).

Each probe has its specific measuring characteristic, which depends on the probe geometry, manufacturing inaccuracies and other influencing parameters. In order to obtain the best possible measuring accuracy, each probe has to be calibrated individually in a well-known flow. For this purpose, the probe is installed in a calibration wind tunnel, where the Mach number and the flow angles are varied systematically, and the five pressures are measured for the different operating conditions. Each Mach number and angle setting is characterized by a set of pressure readings. The relationship between the measured pressure values and the flow properties can be described by normalized coefficients. These parameters which have to be independent from each other are chosen in such a way that they display the abovementioned characteristics. One possibility for the definition of characteristic variables is shown in the following [1]:

$$k_{Ma} = \frac{\Delta p}{p_0} \tag{1}$$

$$k_{\alpha} = \frac{p_3 - p_1}{\Delta p} \tag{2}$$

$$k_{\gamma} = \frac{p_4 - p_1}{\Delta p} \tag{3}$$

with $\Delta p = p_0 - \frac{p_1+p_3}{2}$.

Each calibration parameter is then described by the following function:

* Corresponding author.
E-mail address: homam.nikpey@uis.no (H. Nikpey Somehsaraei).

https://doi.org/10.1016/j.flowmeasinst.2020.101739
Received 9 July 2019; Received in revised form 29 February 2020; Accepted 22 March 2020
Available online 10 April 2020

Nomenclature

AI	Artificial intelligence
ANN	Artificial neural network
$\vec{c}$	Velocity vector
C	Polynomial coefficient
CAD	Computer aided design
GFF	Generalized feed forward
k	Pressure coefficient
MLP	Multilayer perceptron
MAE	Mean absolute error
Ma	Mach number
p	Pressure
Qprop	Quick propagation
R	Correlation factor
RBF	Radial basis function
Rprop	Resilient backpropagation
w	Synaptic weights
x	ANN inputs
y	ANN outputs
Y	Calibration parameter

Greek Symbols

α	Yaw angle
γ	Pitch angle
Δ	Difference
ϕ	Transfer function of the hidden neuron
g	Transfer function of the output neurons

Subscript

ct	Calibration
s	Static
t	Total
0 … 1	Number of pressure holes

$$Y = f(k_{\mathrm{Ma}}, \quad k_{\alpha}, k_{\gamma}) \tag{4}$$

where Y represents calibration parameters, namely Mach number (Ma), yaw angle (α) and pitch angle (γ). In addition, two calibration parameters for the total and static pressures can be defined as:

$$k_{\mathrm{pt}} = \frac{\mathrm{p_t} - \mathrm{p_0}}{\Delta \mathrm{p}} \tag{5}$$

$$k_{\mathrm{ps}} = \frac{\mathrm{p_0} - \mathrm{p_s}}{\Delta \mathrm{p}} \tag{6}$$

The dependencies between the calibration parameters and the three characteristic variables k_{Ma}, k_{α} and k_{γ} are given by the sample points in the calibration space and can be expressed by calibration functions according to Equation (4). Bohn and Simon [1] describe a polynomial approach for the evaluation of the calibration maps for a 5-hole probe with the geometry shown in Fig. 1. A polynomial method for the application with seven-hole probes was published by Gallington [2] and Gerner et al. [3]. The probe head was divided into several sectors accounting for the flow direction. For each of these sectors, four equations for the flow angles, α and γ, as well as the pressure coefficients C_{pt} (total pressure) and C_{q} (dynamic pressure) were defined. Based on the calibration data within one sector, the polynomial coefficients, c, are derived applying a least-squares method for each calibration parameter. The accuracy of this method is sufficient for the center sector (flow direction approximately aligned with probe head axis) but quite poor for the others. Angle errors in the outer sectors increase significantly and are not sufficient for an appropriate application of this approximation approach. Wenger and Devenport [4] reported on an extended approach where they apply error look-up tables for improving the approximation accuracy. In a first step, the calibration functions for the different flow properties are fitted by cubical polynomial functions using the least-square method as describe above. Since the fitting surface results in deviations at the sample points from the calibration, an error value can be derived for each of these points. The calibration function can then be defined as $C(C_{\mathrm{a}},C_{\mathrm{b}}) = f(C_{\mathrm{a}},C_{\mathrm{b}}) + e(C_{\mathrm{a}}, C_{\mathrm{b}})$, where $f(C_{\mathrm{a}}, C_{\mathrm{b}})$ is the polynomial function for each calibration parameter and $e(C_{\mathrm{a}}, C_{\mathrm{b}})$ characterizes the deviations between measurement and approximation at each sample point. The derived error values are listed in a database and can be used for correction of the approximated parameters. For points between the sample points, the errors are derived by interpolation. This method has a significant advantage in comparison to a pure polynomial approach. The application of the polynomial function reduces the interpolation parts and thus the arising interpolation error. Finally, this method provides an exact match with the calibration data.

However, the accuracy of the methods described above significantly depends on the number of sample points during the calibration and the order of the polynomial functions. High-order polynomial functions suffer from overfitting when interpolating between points and on the other hand, low-order polynomial functions cause high deviations at the sample points. Additionally, the number of sample points is directly related to the duration of the calibration involving personal and operational costs. Advanced data analytics based on artificial intelligence (AI) seem to be a promising solution to avoid these limitations while maintaining the desired level of accuracy.

It is well known that ANN as an AI based technique, due to its many advantages such as pattern recognition, nonlinearity and adaptivity [5],

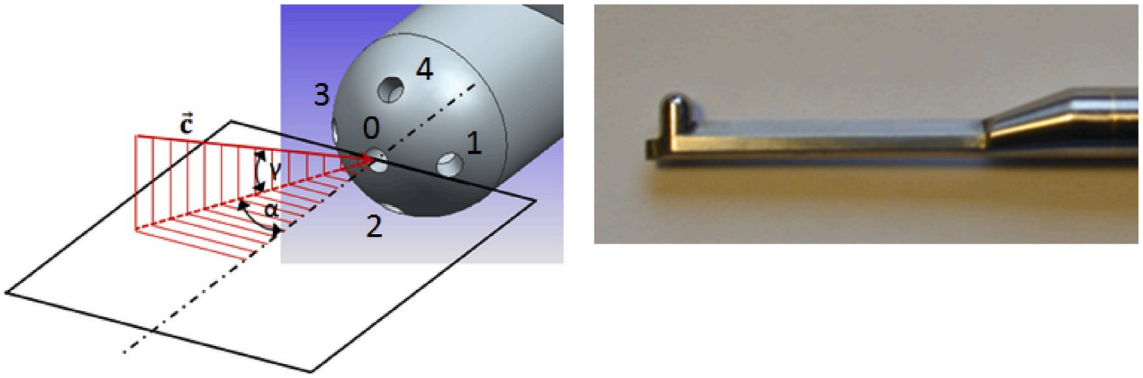

Fig. 1. 5-hole probe (left: CAD model with numbering of the pressure holes, right: probe head with 2.8 mm diameter).

offers a high interpolation capability as well as accurate predictions against unseen data. The ANN learns from the data by constructing a function that relates inputs to outputs. It was shown in authors' previous works that ANN is a suitable method for complex and multidimensional problems [6–10]. Despite several studies focusing on well-stablished approaches such as those mentioned above, there are quite a few publications on the subject of ANN applications for probe calibration. For example, an ANN was used by Rediniotis and Chrysanthakopoulos [11] to predict the flow angles as well as static and total pressure coefficients of a seven-hole probe. The comparison between the predicted and actual values showed that the ANN could not meet the expected accuracy levels and further modifications were required to enhance its performance [11]. As a continuation to this study, Rediniotis together with Vijayagopal [12] developed a self-optimizing ANN based algorithm for calibration of miniature multi-hole probes, which allowed selection of different activation functions for each processing unit or neuron. This resulted in a significant improvement in the prediction accuracies of flow angles and velocities. Fan et al. [13] proposed an ANN based calibration method which was trained using the differential evolution algorithm. The algorithm was developed and tested by limited number of samples obtained from calibrating a five-hole probe. The testing results showed that although ANNs can predict the flow parameters with good accuracy, the deviation between predictions and targets for some samples were still too high [13]. In these studies, the ANNs have shown the potential to provide accurate approximations in probe calibration applications but still more research is required to shed light on the ANN capabilities and achieve more accurate results.

Therefore, this study aims at a detailed investigation on using ANNs for prediction of the calibration parameters of pneumatic multi-hole probes. This was enabled thanks to availability of real-case data from the calibration of a 5-hole probe at the Institute of Jet Propulsion and Turbomachinery, RWTH Aachen University (IST). The final target of these investigations was to explore the possibility to reduce the experimental effort for the calibration by using ANNs for the generation of the calibration maps. Therefore, it was first of all necessary to develop a suitable ANN and to compare the outputs with those from the polynomial approach to make sure that the resulting errors of both methods are in the same order. This could be the basis for future investigations about the effects of reduced number of sample (measuring) points on the accuracy of the ANN.

A systematic analysis in different steps was carried out to identify the optimum network structure. Several networks with different configurations were developed and their performance was evaluated and compared with polynomial functions. The concluding optimum ANN model was then used to develop a novel two-stage approach that resulted in further improvement of the prediction accuracy. Finally, ANNs trained with reduced number of calibration points were used for prediction of the intermediate samples to analyze their interpolation capability. Toward this end, the development and analysis carried out can be summarized as follows:

1. A baseline MLP neural network was trained and tested using calibration data.
2. A systematic analysis through testing different combinations of network, training algorithms, transfer functions and hidden neurons was carried out to find the optimum solution in comparison with the baseline network.
3. The optimum network architecture was then used to develop a two-stage approximation approach that incorporated two ANNs to predict the calibration parameters and the approximation errors separately. The sum of the predictions of two ANNs gives the estimation of the measured value.
4. Finally, to test the interpolation capability of the ANNs, the proposed two-stage method was tested by data at the intermediate points between two sample points, which were not used during training.

The paper is organized as follows. In Section 2, the methodology, including experimental setup, polynomial and ANN approaches used in this study is described. The detailed discussions on the obtained results are presented in Section 3, which is then followed by the conclusion in Section 4.

2. Methodology

2.1. Experimental setup

For the generation of a database for the comparison of the two approximation procedures, a spherical 5-hole probe (see Fig. 1) was calibrated in a free stream wind tunnel at ambient conditions for a Mach number range between 0.1 and 0.8. Fig. 2 shows a typical calibration set-up. The probe positioning and high accuracy angle adjustment was performed by means of a robot. The probe was positioned stepwise in different angle settings in the range of ±25° in yaw and in pitch direction. In the normal calibration process, the steps are chosen to 5°.

Fig. 3 shows an example of a calibration map for the abovementioned angle range and steps of 5°. The distributions of the characteristic variables k_α and k_γ for $\alpha = 0°$ and for $\gamma = 0°$ are almost horizontal and vertical lines which indicate a high manufacturing accuracy with good geometric symmetry. However, it becomes obvious that for high angles of attack the surface becomes quite destorted. The deformation of the lines in the center region of k_α indicate the influence of the probe stem at high pitch angles (see angle definition in Fig. 1). This asymmetric behavior means a significant challenge for a proper surface fitting with low approximation errors.

2.2. Polynomial function approach

As a commonly applied approach, the mathematical relationship between the three characteristic variables k_α, k_γ and k_{Ma} and the flow parameters is established by multi-parametric approximations:

$$Y = \sum_{i=0}^{l} \sum_{j=0}^{m} \sum_{k=0}^{n} \delta_{i,j,k} \cdot C_{Y\ i,j,k} \cdot k_{Ma}^{k} \cdot k_{\alpha}^{j} \cdot k_{\gamma}^{i} \tag{7}$$

with

$$\delta_{i,j,k} = \begin{cases} 1 & \text{if } i,\ j,\ k \le \max(l,\ m,\ n) \\ 0 & \text{for the other cases} \end{cases}$$

The polynomial degrees l, m and n are usually not the same. In the evaluation process for the calibration data, they are varied between three and the maximum degree. The coefficients $C_{Y\ i,j,k}$ are determined by applying the least square method.

Considering the abovementioned calibration range ($0.1 < Ma < 0.8$ in steps of $\Delta Ma = 0.1$, $\alpha = \pm 25°$ in steps of $\Delta\alpha = 5°$, $\gamma = \pm 25°$ in steps of $\Delta\gamma = 5°$), in total 968 data sets (Y, k_{Ma}, k_α, k_γ) are available for the approximation. For each calibration coefficient (calibration map), one polynomial (fitting function) is derived. Due to the imperfectness of the calibration maps described above, certain deviations between the measured sample points and the approximation values will occur. Fig. 4 shows these approximation errors at the example of the Mach number. The left diagram indicates the deviations at each sample point. The error histogram in the right diagram demonstrates that in about 70% of the points, the differences between approximated and measured Mach numbers (ΔMa) is less than 0.0055 (i.e. almost 1%). The maximum deviation is 0.016 and the average value was calculated to 0.004.

In addition to the deviations at the calibration points, the polynomial functions may show unwanted oscillations between the sample points. These may lead to significant errors in the calculated flow properties. Fig. 5 illustrates this problem on the calibration surfaces at $Ma = 0.5$ for the yaw and pitch angle as well as the Mach number and the coefficient k_{pt}. These diagrams show the regarding calibration as well as several

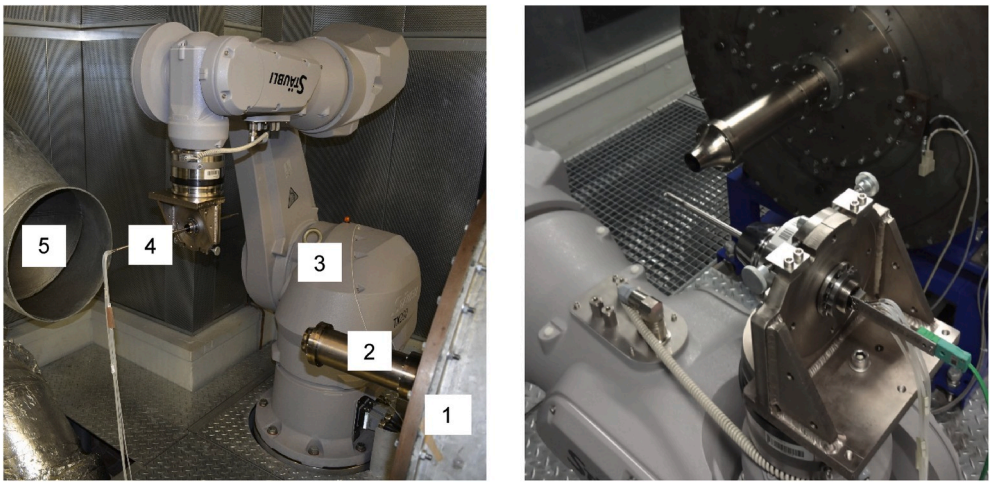

Fig. 2. Calibration wind tunnel with robot (left: total view, right: probe in front of nozzle). The components of the wind tunnel shown in the picture are 1. Settling chamber, 2. Nozzle, 3. Robot, 4. Probe and 5. Exhaust duct.

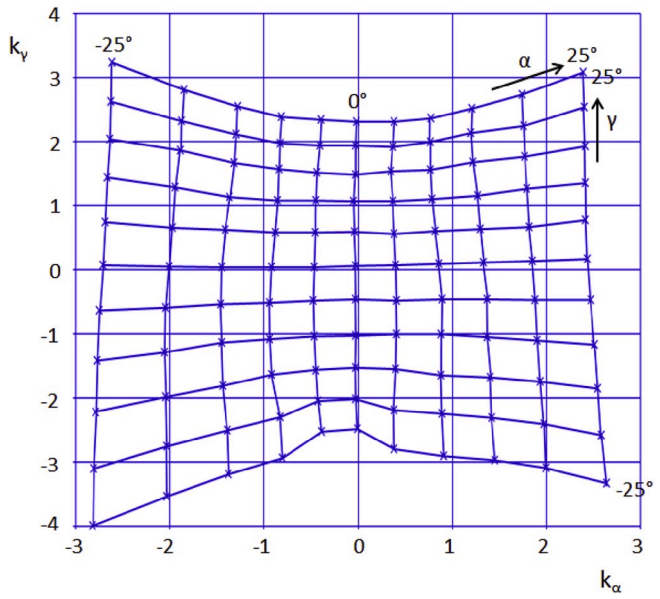

Fig. 3. 2D calibration map $k_\alpha - k_\gamma$ for $Ma = 0.55$.

points indicating errors of the flow values at intermediate points between two sample points. For this, the results from the polynomial function were compared to linearly interpolated points in the k_α-k_γ plane. Orange interpolation points indicate a medium deviation and red interpolation points denote a high deviation from the expected calibration surface. Interpolated points with low deviations are not displayed. Fig. 5a and b shows the yaw angle, α, and the pitch angle, γ, respectively. Orange points indicate deviations larger than 0.3°, red points larger than 0.5°. The yaw angle exhibits large deviations in the region of large positive values of k_α and k_γ. Likewise, the pitch angle shows high deviations in the region of large positive k_α values as well as in the region of large negative k_α values in combination with large positive k_γ values. Similarly, the Mach number as well as the coefficient k_{ps} in Fig. 5c and d displays significant deviations due to oscillations of the polynomial functions. Orange interpolation points indicate deviations larger than 0.0025 Ma and 0.015 k_{ps}, red interpolation points represent deviations larger than 0.005 Ma and 0.025 k_{ps}.

The risk of these oscillations increases with the order of the polynomial functions. However, higher order polynomials usually minimize the deviations at the calibration points. Since such oscillations are in general unpreventable using polynomial functions, advanced analytics like ANN should be favored.

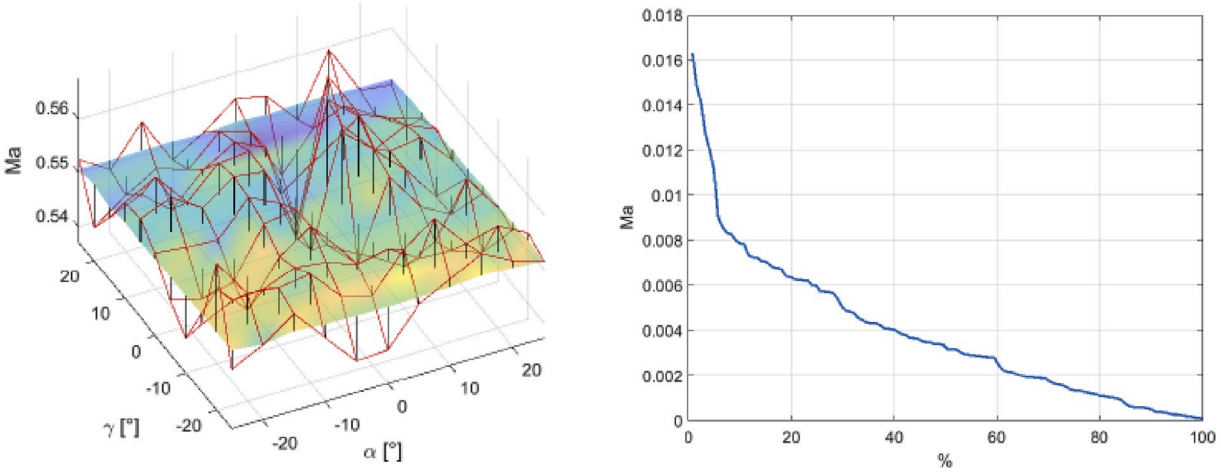

Fig. 4. Approximation error for $Ma = 0.55$ (left: deviations at the sample points, right: error histogram).

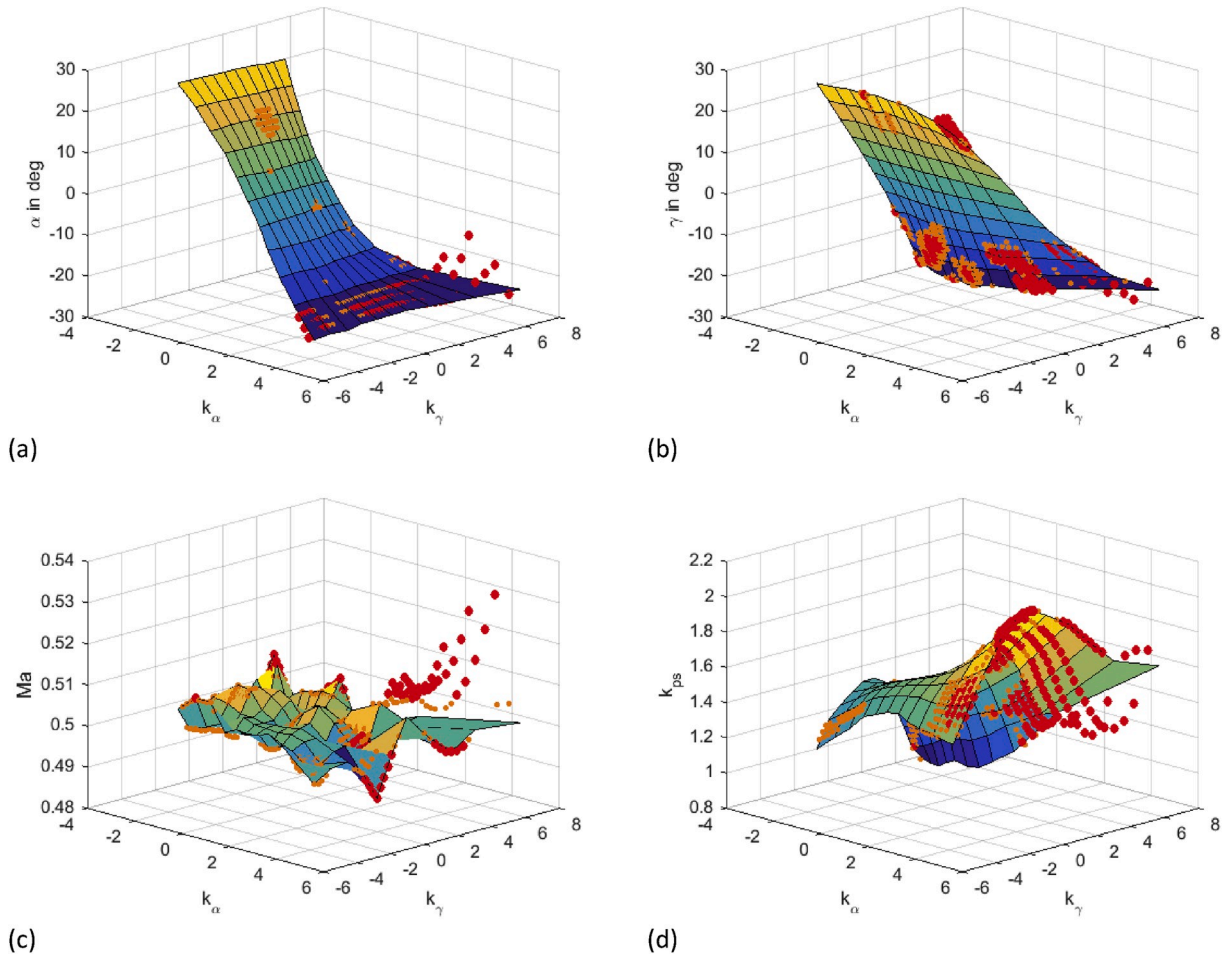

Fig. 5. Visualization of polynomial oscillations between calibration points for $Ma = 0.5$ as a function of k_α and k_γ.(a) α angle, (b) γ angle, (c) Mach number, (d) calibration parameter k_{ps}.

2.3. ANN based approach

The ANN mimics the way in which the brain performs. It mainly consists of processing units called artificial neurons that are connected to each other to form the structure or topology of the network. The neurons contain an activation or a transfer function that transforms the input signals to output signals. The neural network learns the knowledge about a system, which is represented by a data set, through a training process. During the training process, the interneuron connections, so-called synaptic weights or weights, are tuned to store the salient features that characterize the data [5]. Once ANNs are trained, the weights are frozen, and the long-term memory of the ANN is formed. The trained ANN enables the acquired knowledge to be recalled predicting the outputs when new inputs are introduced. The ANN usually performs accurately for data lying in between the training data, which is indeed referred to high interpolation capability of a trained ANN.

Like the polynomial function approach, as shown in Fig. 6, the ANN was constructed to approximate calibration parameters including *Ma*, α, γ, k_{pt} and k_{ps} as a function of characteristic variables, namely k_α, k_γ and k_{Ma}. A data set consisting of 9680 measurements from 986 calibration points (as described in preceding section) with 10 measurements at each calibration point was used to train the ANN model. The arithmetically averaged measured values at each calibration point, constituting a data set with 968 samples, were used for testing the performance of the trained networks. For better understanding, Table 1 shows an example of training and testing samples at a particular calibration point (i.e. at $Ma = 0.5$, $\alpha = 10^\circ$ and $\gamma = 25^\circ$).

There are different parameters such as the neural network structure,

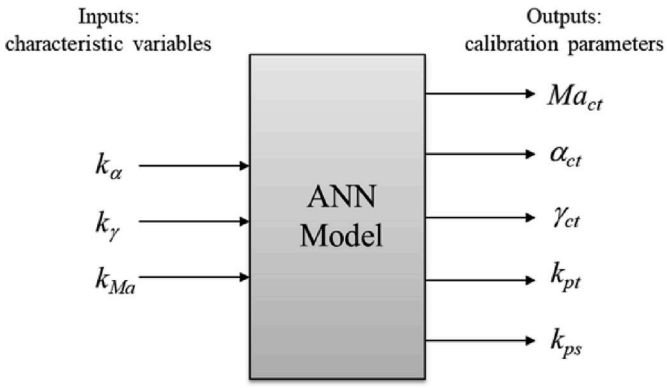

Fig. 6. ANN model structure.

training algorithm, and transfer function that should be optimized in developing an ANN model. Optimizing these parameters involves developers' experience as well as trial and error, which requires systematic testing of various options and retraining to identify the best combination. The approach used in this study will be explained in detail in the rest of the section.

Previous experiences of authors show that feed-forward network architectures have been a suitable method for the modeling of complex energy systems when an accurate prediction is required [6–10]. Of these networks, the multilayer perceptron (MLP) is by far the most commonly

Table 1
An example of training and testing samples.

no. Measurements	α_{ct}	γ_{ct}	Ma_{ct}	k_{α}	k_{γ}	k_{Ma}	k_{pt}	k_{ps}
1	10	25	0.5	−1.015	−2.026	0.091	0.481	1.326
2	10	25	0.5	−1.013	−2.023	0.091	0.478	1.326
3	10	25	0.5	−1.014	−2.024	0.091	0.479	1.326
4	10	25	0.5	−1.014	−2.025	0.091	0.483	1.326
5	10	25	0.5	−1.014	−2.024	0.091	0.478	1.326
6	10	25	0.5	−1.014	−2.027	0.091	0.480	1.327
7	10	25	0.5	−1.017	−2.021	0.091	0.478	1.325
8	10	25	0.5	−1.017	−2.024	0.091	0.478	1.325
9	10	25	0.5	−1.017	−2.024	0.091	0.481	1.326
10	10	25	0.5	−1.017	−2.029	0.091	0.481	1.327
Averaged value for testing	10	25	0.5	−1.015	−2.025	0.091	0.480	1.326

applied network. Fig. 7 shows a typical MLP structure with one hidden layer. The inputs denoted by x are multiplied by weights, which represent the strengths of connections connecting input units to neurons in the hidden layer. The weighted inputs are then summed and transformed while passing through the hidden neurons. The outputs of hidden neurons are the inputs for the output layer. They are weighted, combined and processed in the hidden layer, where the outputs corresponding to inputs are calculated. The functional representation of an MLP network with n inputs, k hidden neurons and m outputs shown in Fig. 7 can be defined using Equation (8):

$$y_m = g\left(\sum_{j=0}^{k} w_{mj}^{2}\phi\left(\sum_{i=0}^{n} w_{ji}^{1}x_i\right)\right) \tag{8}$$

w_{ji}^{1} is a weight connecting input i to the hidden unit j, and w_{j0}^{1} is the bias for the hidden unit j, corresponding to the fixed input x_0 equals 1. Similarly, w_{mj}^{2} denotes a weight, connecting hidden unit j to the output unit m, and w_{m0}^{2} is the bias for the output unit m, corresponding to the fixed input equals 1. $\phi(.)$ and $g(.)$ represent the transfer function of the hidden and output neurons respectively.

As the first attempt, an MLP neural network with one hidden layer was evolved during the training process. The training process of MLPs is carried out in two phases. Firstly, errors are evaluated in the output layer and weights between the output and the hidden layer (w_{mj}^{2}) are adjusted. Secondly, the resulting error is propagated in a backward path through the network, and weights between the hidden layer and the input layer (w_{ji}^{1}) are updated. This process is repeated until the error between the predicted outputs and desired values is converged to an acceptable low level. This algorithm is known as back-propagation [5]. Although MLPs can have more than one hidden layer, there is no impediment to having more than one hidden layer. It has been proved that one layer of the hidden neurons with a continuous activation function is enough to approximate any continuous functions if it has a sufficient number of neurons (i.e. universal approximation theorem) [5]. The sigmoid hyperbolic tangent function was chosen as the transfer function and the number of hidden neurons varied from 10 to 20. The batch method was used for updating the weights. In the batch method, all training examples, known as epoch, are introduced to the network and training is performed on epoch-by-epoch basis. The results illustrated the capability of the ANN to approximate the calibration parameters with rather good accuracy.

The developed MLP was considered as the baseline ANN and various network options and training algorithms were then examined to identify the optimum combination of the network structure, learning algorithm and transfer function. This was carried out systematically in a three-step trial and error analysis. The first step concerned specifying the most suitable network with highest prediction performance. There are many different types of feed-forward neural networks, but most of them can be classified as belonging to one of the main networks, namely MLP, generalized feed forward (GFF), Jordan-Elman and radial basis function (RBF) networks. Different ANNs based on these networks were trained using the abovementioned settings and their accuracies were tested and compared with each other. Fig. 8 shows the results of selecting different network structures. MLP emerged as the best network with lowest approximation error for all calibration parameters. In the second step, the prediction performance of MLP network was investigated with different learning algorithms in order to find the most compatible learning algorithms. Fig. 9 presents the approximation errors for output

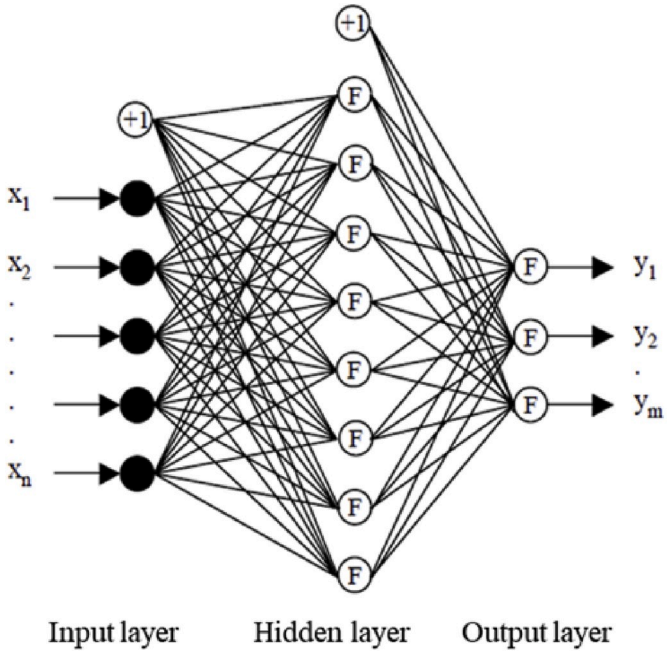

Fig. 7. Schematic of a MLP network [14].

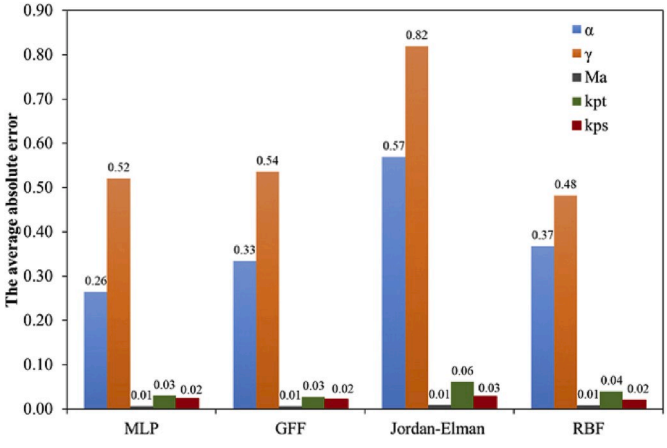

Fig. 8. Approximation errors for different networks.

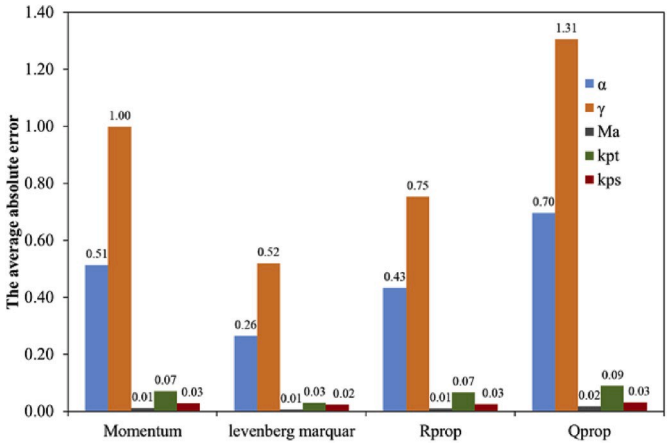

Fig. 9. Approximation errors for different learning algorithms.

parameters with respect to learning algorithms. The results showed that Levenberg–Marquardt (LM) algorithm undoubtedly provides the best prediction results for MLP. Since the MLP training involves back propagation of errors, the neurons of the hidden layer should have nonlinear transfer functions, but neurons in output layer can have either linear or nonlinear functions. The sigmoidal nonlinear function is a commonly used transfer function in the design of MLPs, two main forms of which are the logistic and hyperbolic tangent (*tanh*) functions. The third step of analysis aimed at defining the most desired transfer function. After testing different functions, nonlinear *tanh* was selected for both hidden and output layers.

The results of the systematic analysis showed that the MLP network with *tanh* transfer function, which was trained by LM algorithm, provides the least amount of approximation errors. Nevertheless, the errors were still higher than those that were obtained from the polynomial function approach. Variations in the number of hidden neurons using 25, 30, 35, 40, 45 and 50 neurons were promoted and it was found that the MLP with 50 hidden neurons increases the accuracy, without losing the generalization or prediction capability. Higher numbers of hidden neurons were also tested but no further improvement in approximation errors was achieved.

Given the limited accuracy of the MLP, a novel two-stage approximation approach was thus proposed to improve the results. This approach involved two MLPs with the optimum architecture obtained from analysis as discussed above to approximate the calibration parameters and the approximation errors separately. Fig. 10 shows the sketch of the two-stage approach. The first MLP was used to predict the calibration parameters. The errors ($\hat{e}_i$) generated by comparison

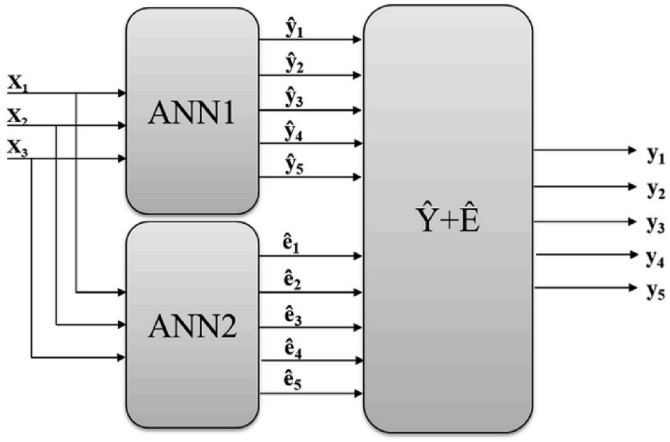

Fig. 10. The schematic of two-stage approximation approach.

between predictions and desired values were then used to form an error data set. The error data set was used to train the second MLP, providing an estimation of the error for the same set of inputs. Since the developed approach should be able to predict the output parameters in the unknown flow and thus the input parameters should be independent of the flow parameters, the same input parameters were used in ANN2 to predict the errors. The final approximation is obtained by the summation of the results from both ANNs, i.e. $\hat{Y} + \hat{E}$. The ANN model derived from error values was used for refining the approximated parameters. It was found that the approximation accuracy was further improved using the proposed two-stage approach. The obtained results were in agreement with the study reported in Ref. [4], where two polynomial functions were used to approximate the parameters and errors. Finally, the interpolation capability of the two-stage method was tested using a data set that contained samples at intermediate flow angles (α and γ from −25 to 25 with step of 1.25°) for the same Mach numbers used for the calibration. The results obtained from the performed analyses are presented and discussed in the next section.

3. Results and discussions

This section presents and discusses the results in detail. Two main parameters, namely correlation factor (R) and mean absolute error (MAE), were considered to assess and compare the performance of the developed ANNs. They are defined as following:

$$\mathrm{MAE} = \frac{\sum_{i=1}^{N} |\hat{y}_i - y_i|}{N} \tag{9}$$

$$R = \frac{\sum_{i=1}^{N} (\hat{y}_i - \overline{\hat{Y}})(y_i - \overline{Y})}{\sqrt{\sum_{i=1}^{N} (\hat{y}_i - \overline{\hat{Y}})^2 \sum_{i=1}^{N} (\hat{y}_i - \overline{Y})^2}} \tag{10}$$

where $\hat{y}_i$ and y_i represent the ith approximated and measured values of a particular calibration parameter, $\overline{\hat{Y}}$ and $\overline{Y}$ are respectively the average of approximated and measured values of that calibration parameter. N denotes the number of samples. The correlation factor R is a measure of the linear relationship between prediction and desired values. The greater the R is, the better the model fits to the data. The MAE is a measure for the accuracy of the models, which is defined by the mean absolute error between the predicted and desired values. The smaller the MAE is, the more accurate the model is.

Table 2 shows the approximation errors of calibration parameters that resulted from the optimum single-stage ANN in comparison with the errors obtained from the polynomial approximation. It can be seen that the levels of errors for all output parameters are considerably low and the accuracies of most outputs are approximately at the same level as the polynomial approach. However, the maximum errors are slightly higher than those of polynomials. The linear correlation coefficient, R, for flow parameters and pressure coefficients is almost around 0.999, which indicates that the predictions are very close to measurements.

Due to the fact that a high level of accuracy is required for the calibration, the two-stage method based on ANN as shown in Fig. 10 was proposed and developed to enhance the performance of the approximation task. The approximation errors of outputs are listed in Table 3. The results generally show that the errors are further reduced using the proposed methods, which was also noticed with the slight improvement in R coefficient for all output parameters. More specifically, not only the MAE of α_{ct}, Ma_{ct} and k_{pt} are similar to the polynomial approach but also the maximum deviation decreased. For γ_{ct} and k_{ps}, the MAE decreased but the maximum error is still a little higher compared to the polynomial approximation. The high value of R, i.e. 0.999, achieved for all output parameters, indicates a very good match between predicted and measured values. This is illustrated in Fig. 11, where the approximated values (y-axis) are plotted together with desired values (x-axis) for all outputs. The dashed line is the best-fit line that represents the best linear

Table 2
The approximation errors of calibration parameters for the optimum single-stage ANN architecture.

Outputs	ANN MAE	ANN Max. error	R	Polynomial MAE	Polynomial Max. error	Polynomial R
α_{ct}	0.129	0.597	0.999	0.090	0.600	0.999
γ_{ct}	0.233	1.267	0.999	0.130	0.910	0.999
Ma_{ct}	0.002	0.022	0.999	0.002	0.014	0.999
k_{pt}	0.012	0.085	0.999	0.009	0.076	0.999
k_{ps}	0.010	0.065	0.997	0.006	0.040	0.991

Table 3
The approximation errors of calibration parameters for the two-stage ANN method.

Outputs	ANN MAE	ANN Max. error	R	Polynomial MAE	Polynomial Max. error	Polynomial R
α_{ct}	0.087	0.437	0.999	0.090	0.600	0.999
γ_{ct}	0.194	1.375	0.999	0.130	0.910	0.999
Ma_{ct}	0.002	0.013	0.999	0.002	0.014	0.999
k_{pt}	0.010	0.071	0.999	0.009	0.076	0.999
k_{ps}	0.009	0.057	0.999	0.006	0.040	0.991

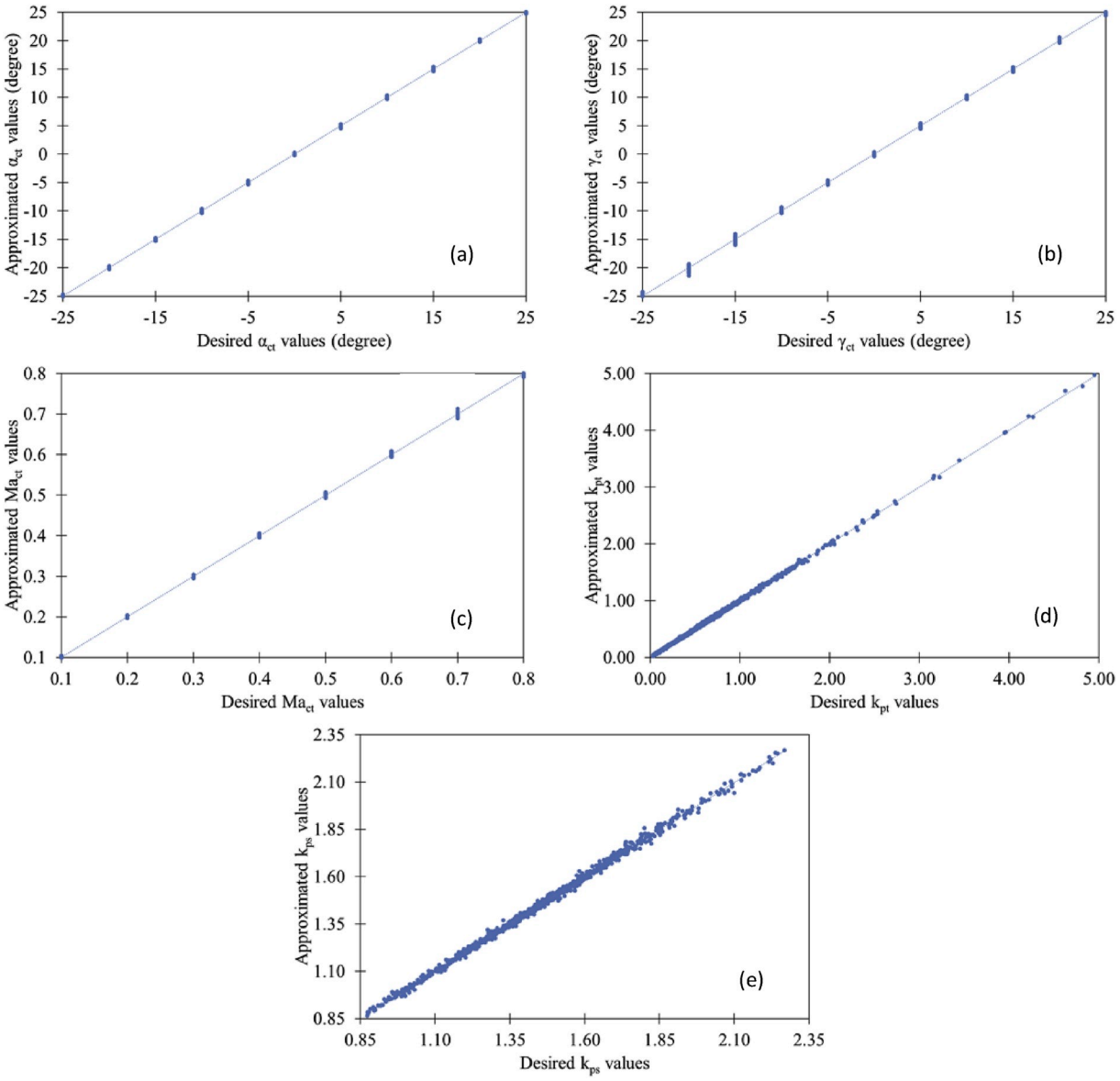

Fig. 11. Comparison between the desired and approximated (a) α_{ct} (b) γ_{ct} (c) Ma_{ct} (d) k_{pt} and (e) k_{ps} values using two-stage ANN method.

relationships between predictions and measurements. It can be seen that the predicted values fit to the measured values, with almost all data lying on a straight line.

In order to determine the flow parameters for total and static pressure (p_t and p_s), the predicted k_{pt} and k_{ps} values are further processed using Equations (5) and (6). Their values were compared with those from the polynomial approach. The approximation error and the error distribution over different ranges for these two parameters together with α_{ct}, γ_{ct} and Ma_{ct} are shown in Table 4. While the approximation errors for α_{ct}, Ma_{ct} and p_s have improved using ANN, polynomial approximations provide better results for p_t and γ_{ct}. However, the differences are small and generally, the performance of the two approaches is quite comparable.

An ANN trained with the data for a particular range is in general able to predict output parameters with good accuracy for a different range lying in between the ranges of training data. This is called the interpolation capability of the ANN. To check the interpolation capability of the two-stage ANN approach, the calibration data at $Ma = 0.5$ is linearly interpolated to generate three intermediate points in each direction of the k_α- and k_γ-plane. This results in an interpolated grid with steps of 1.25° in the yaw and pitch angle direction, as shown in Fig. 12. On the basis of the interpolated calibration variables, the polynomial functions and the trained two-stage ANN were used to predict the calibration parameters at the interpolated points. The linearly interpolated calibration parameters were used as a reference to determine the performance for each approach. Although this procedure assumes that the distribution of the intermediate points exhibits a purely linear behavior, it can be used to check the general interpolation capabilities. Table 5 lists results of the interpolation study for the two-stage ANN approach and the polynomial functions at $Ma = 0.5$. The values for the mean absolute errors are comparable between the ANN and the polynomial functions. However, the ANN performs much better for the maximum errors. Moreover, for flow angles, the ANN provides a clear advantage. As a result, the two-stage ANN approach is the preferred algorithm due to its better interpolation capabilities. For better illustration, the scatter plots of the ANN and polynomial predictions with respect to reference values for flow angles are provided in Fig. 13. The red markers represent the polynomial approximations, which show undesired deviations at some intermediate points.

Unlike the polynomial approximation, which is highly dependent on the data and shows large deviations at intermediate samples, the proposed ANN based approach provides satisfactory results at intermediate points without being overfitted to training data. In other words, if these two approaches were used to interpolate in ranges falling between the calibration points, the ANN approach can make much better predictions.

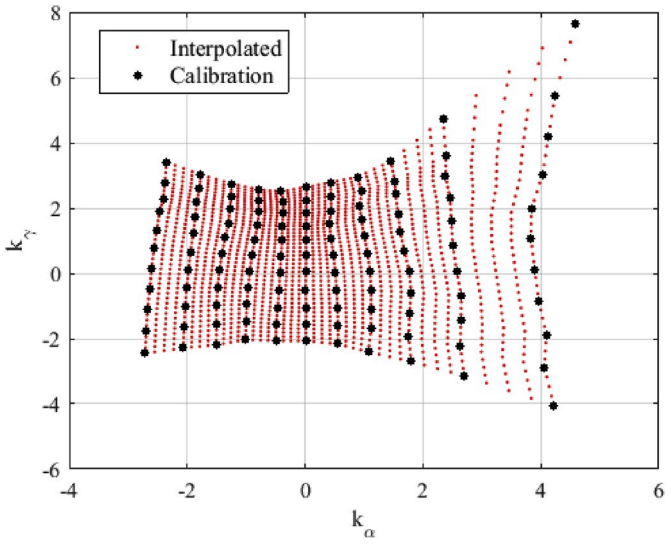

Fig. 12. Calibration grid and linearly interpolated grid at $Ma = 0.5$.

Table 5
The approximation errors of calibration parameters for interpolation study.

Outputs	ANN MAE	ANN Max. error	Polynomial MAE	Polynomial Max. error
$\boldsymbol{\alpha_{ct}}$	0.138	1.625	0.168	10.475
$\boldsymbol{\gamma_{ct}}$	0.247	1.698	0.198	2.874
$\boldsymbol{Ma_{ct}}$	0.003	0.032	0.002	0.029
$\boldsymbol{k_{pt}}$	0.012	0.188	0.012	0.233
$\boldsymbol{k_{ps}}$	0.016	0.290	0.013	0.306

4. Conclusion

In this study, the application of the ANN to predict the flow parameters for calibration of multi-hole pressure probes was investigated and compared with the commonly used polynomial functions. For this purpose, the data obtained from the calibration of a five-hole probe with spherical head at the Institute of Jet Propulsion and Turbomachinery, RWTH Aachen University (IST) was used to develop ANNs and test their performance. A baseline ANN was constructed and then the network architecture and setup was optimized through a systematic four-step analysis by examining different combinations of network options, learning algorithms, transfer function and number of neurons in the hidden layer. It was concluded that the MLP network with one hidden layer and nonlinear transfer function for both hidden and output

Table 4
The approximation errors and error distribution of calibration parameters for the two-stage ANN method.

Error range	<0.1°	0.1°–0.2°	0.2°–0.3°	0.3°–0.4°	0.4°–0.5°	>0.5°		
α_{ct} - poly	640	228	77	13	7	3		
α_{ct} -ANN	638	247	67	15	1	0		
γ_{ct} - poly	540	225	105	52	20	26		
γ_{ct} - ANN	331	254	185	98	45	55		
Error range	**< 0.001**	**0.001–0.002**	**0.002–0.003**	**0.003–0.004**	**0.004–0.005**	**> 0.005**		
Ma_{ct} - poly	215	337	207	111	50	48		
Ma_{ct} - ANN	435	281	119	68	40	25		
Error range	**< 50 Pa**	**50–100 Pa**	**100–150 Pa**	**150–200 Pa**	**200–550 Pa**	**> 250 Pa**	**Max. Error**	**MAE**
p_t - poly	684	154	58	19	22	31	532	48
p_t - ANN	526	161	99	51	32	99	1034	91
p_s - poly	544	146	100	50	41	87	1026	85
p_s - ANN	565	151	85	56	41	70	833	79

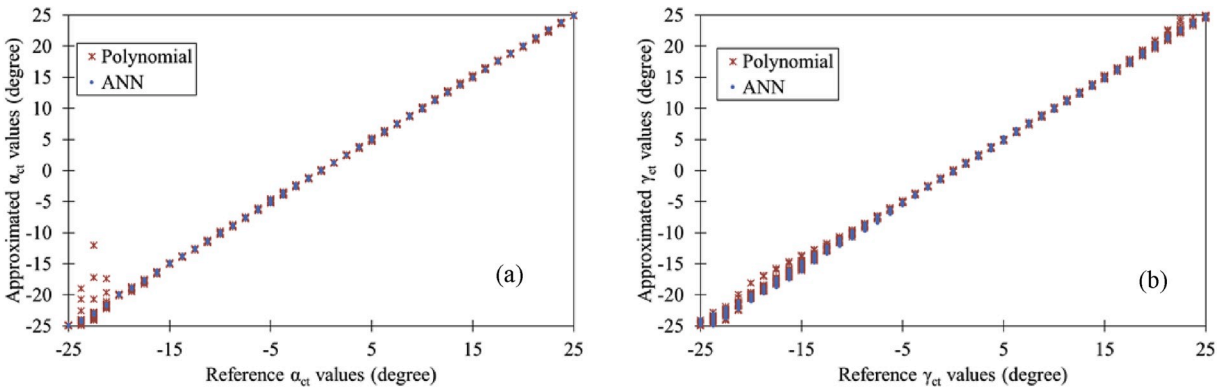

Fig. 13. Comparison between the reference and approximated (a) α_{ct} (b) γ_{ct} values using two-stage ANN method and polynomial at intermediate samples.

neurons, which was trained by Levenberg–Marquardt algorithm, provides the optimum solution with best accuracy compared to the polynomial approach. The MAE for outputs, namely Ma_{ct}, α_{ct}, γ_{ct}, k_{pt} and k_{ps}, are 0.129, 0.233, 0.002, 0.012 and 0.01, respectively, which are comparable to the accuracy of the polynomial approach. The optimum ANN setup was used to develop a novel two-stage ANN method. First, the flow parameters were predicted and then an error data set was generated by calculating the errors between predictions and measurements to develop the second ANN, providing an estimation of the error for the same inputs. The final outputs are calculated by the sum of the predictions of flow parameters and corresponding error values. The validation results showed that the approximation accuracy was further improved using the proposed two-stage approach. While for the α_{ct}, Ma_{ct} and k_{pt}, the error levels were at the same levels as the polynomial approximations, the MAE of γ_{ct} and k_{ps} decreased and a very high value of R i.e. 0.999 was achieved for all output parameters. Finally, the interpolation capability of the two-stage ANN approach was studied using linearly interpolated points. The comparison with the polynomial functions illustrated that the ANN method proposed in this study not only predicts the flow parameters with high accuracy comparable to the polynomial functions at the calibration points, but also performs better at intermediate points. The maximum error for α_{ct} and γ_{ct} significantly reduced from 10.475 to 2.874 to 1.625 and 1.698, respectively. The results basically showed that ANN with high interpolation capability provides the potential to reduce the experimental efforts, and thereby the cost, for the generation of the calibration maps, using less sampling points. In this context, the future work of the authors mainly focuses on evaluating the effects of reduced number of sample (measuring) points on the accuracy of the ANN.

Author statement

All persons who meet authorship criteria are listed as authors, and all authors certify that they have participated sufficiently in the work to take public responsibility for the content, including participation in the concept, design, analysis, writing, or revision of the manuscript.

Declaration of competing interest

The authors declare that they have no known competing financial interests or personal relationships that could have appeared to influence the work reported in this paper.

References

[1] D. Bohn, H. Simon, Mehrparametrige Approximation der Eichräume und Eichflächen von Unterschall- bzw. Überschall-5-Loch-Sonden, in: Tm - Technisches Messen, 1975, p. 81.
[2] R. Gallington, Measurement of Very Large Flow Angles with Non-nulling Seven-Hole Probes, Aeronautics Digest, USAF Academy, Colorado, 1980, pp. 60–88.
[3] A. Gerner, C. Maurer, R.J.E.i.F. Gallington, Non-nulling seven-hole probes for high angle flow measurement. 2 (2) (1984) 95–103.
[4] C.W. Wenger, W.J.J.A.j. Devenport, Seven-hole pressure probe calibration method utilizing look-up error tables 37 (6) (1999) 675–679.
[5] S.S. Haykin, Neural Networks and Learning Machines, vol. 3, Pearson Education Upper Saddle River, 2009.
[6] M. Fast, M. Assadi, S. De, Development and multi-utility of an ANN model for an industrial gas turbine, Appl. Energy 86 (1) (2009) 9–17.
[7] J. Smrekar, et al., Prediction of power output of a coal-fired power plant by artificial neural network. Neural Computing and Applications 19 (5) (2010) 725–740.
[8] H. Nikpey, M. Assadi, P.J.A.E. Breuhaus, Development of an Optimized Artificial Neural Network Model for Combined Heat and Power Micro Gas Turbines, vol. 108, 2013, pp. 137–148.
[9] H. Nikpey, et al., Experimental Evaluation and ANN Modeling of a Recuperative Micro Gas Turbine Burning Mixtures of Natural Gas and Biogas., vol. 117, 2014, pp. 30–41.
[10] H. Nikpey, et al., Modeling and control of SI engines air-fuel ratio by ensemble of model predictive control, radial basis function neural network, and genetic algorithms, in: INISTA 2009, Trabzon, Turkey, 2009.
[11] O. Rediniotis, G. Chrysanthakopoulos, Application of neural networks and fuzzy logic to the calibration of the seven-hole probe, J. Fluid Eng. 120 (1) (1998) 95–101.
[12] O.K. Rediniotis, R. Vijayagopal, Miniature multihole pressure probes and their neural-network-based calibration, AIAA J. 37 (6) (1999) 666–674.
[13] H.-Y. Fan, et al., An improved neural-network-based calibration method for aerodynamic pressure probes, J. Fluid Eng. 125 (1) (2003) 113–120.
[14] E. Mesbahi, et al., A unique correction technique for evaporative gas turbine (EvGT) parameters, in: ASME Turbo Expo 2001: Power for Land, Sea, and Air, American Society of Mechanical Engineers, 2001.